JACS
JOURNAL OF THE AMERICAN CHEMICAL SOCIETY

Article

pubs.acs.org/JACS

Circular Dichroism Probed by Two-Photon Fluorescence Microscopy in Enantiopure Chiral Polyfluorene Thin Films

Matteo Savoini,[†,∥,⊥] Xiaofei Wu,[‡,∥] Michele Celebrano,[†,∥] Johannes Ziegler,[‡,#] Paolo Biagioni,[†] Stefan C. J. Meskers,[§] Lamberto Duò,[†] Bert Hecht,[‡] and Marco Finazzi*[,†]

[†]CNISM-Dipartimento di Fisica, Politecnico di Milano, Piazza Leonardo da Vinci, 20133 Milano, Italy

[‡]Nano-Optics & Biophotonics Group, Department of Experimental Physics 5, Wilhelm-Conrad-Röntgen-Center for Complex Material Systems (RCCM), Physics Institute, University of Würzburg, Am Hubland, D-97074 Würzburg, Germany

[§]Molecular Materials and Nanosystems, Eindhoven University of Technology, P.O. Box 513, NL 5600 MB Eindhoven, The Netherlands

ABSTRACT: Two-photon fluorescence scanning confocal microscopy sensitive to circular dichroism with a diffraction-limited resolution well below 500 nm is demonstrated. With this method, the spatial variation of the circular dichroism of thermally annealed chiral polyfluorene thin films has been imaged. We observed circular dichroism associated with submicrometer-sized domains showing helicoidally twisted macromolecular organization. Domains with opposite chiroptical properties, corresponding to left- or right-handed molecular organization, coexist in the film. Our results are consistent with those obtained by one-photon imaging and illustrate the potential of two-photon imaging for use in studying helical macromolecular organization.

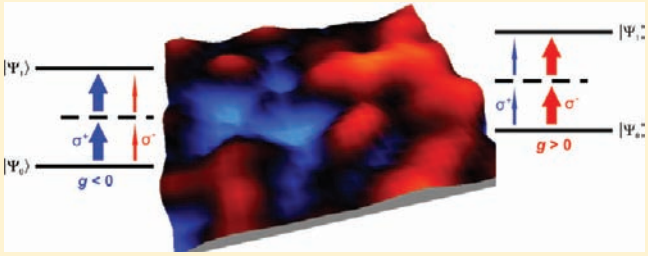

1. INTRODUCTION

Circular dichroism (CD) is the difference in absorbance of left circularly polarized (LCP) and right circularly polarized (RCP) light by chiral molecules or materials. It is sensitive to the helical conformation and organization of molecular assemblies and (bio)polymers. In the last decades, sensitive detection schemes have been developed to measure spatially averaged CD using two-photon transitions,[1−3] for example, via fluorescence-detected CD, two-photon absorption, and two-photon fluorescence (TPF).[4,5] Z-scan[6,7] and L-scan[8] methods have been proven useful in the determination of spectral nonlinear dichroic properties in chiral molecules. These techniques, however, lack the ability to address the CD spatial distribution. Nevertheless, many polymeric and biological samples exhibit CD that strongly varies with position because of intrinsic fluctuations in the sample or formation of ordered domains.[9,10] Adding CD sensitivity to two-photon-based spatially sensitive techniques might thus provide important information about microscopic molecular organization.

Spatially resolved multiphoton microscopy offers several advantages in comparison with single-photon excitation,[11] giving it enormous potential for use in medical and biological sciences.[12] First, the background in 3D imaging is considerably reduced. Second, the light-induced bleaching outside the focal volume is much lower thanks to the low linear absorption of the sample at the excitation photon energy. Other advantages are the reduced scattering because of longer excitation wavelengths and the absence of photoinduced degradation of the sample by scattered excitation light.[11] The fact that a pulsed laser is needed to excite TPF efficiently can also be exploited to obtain information on the intrinsic lifetimes of excited states involved in the fluorescence generation.[13]

In this work, we combined 2D imaging of CD with high-resolution TPF confocal microscopy to map the spatial distribution of the nonlinear CD properties of polymeric samples. To illustrate the potential of CD−TPF microscopy, we studied thin films of a chiral, π-conjugated polyfluorene, poly[9,9-bis((3*S*)-3,7-dimethyloctyl)-2,7-fluorene] (**1**) (Figure 1 inset), that show exceptionally large degrees of CD after thermal annealing.[14] This large CD could be exploited in organic devices.[15,16] During the annealing process at elevated temperature (~390 K), the polyfluorene is brought into its liquid-crystalline state, while subsequent cooling to room temperature freezes the induced molecular arrangement. In a solid film, molecules of **1** show bright blue fluorescence from the lowest excited singlet state, which is ~3 eV above the ground state. This excited level can also be populated via two-photon excitation using a pulsed Ti:sapphire laser source (photon energy of ~1.5 eV).[17,18]

The large single-photon CD observed after annealing of the polymer **1** derives from long-range cholesteric order[19] characterized by the coexistence of domains showing opposite chirality. Because of the presence of chiral side chains, the ground state is the left-handed one, as evidenced by the fact that the balance between opposite-chirality domains varies

Received: November 3, 2011
Published: March 13, 2012

   dx.doi.org/10.1021/ja209916y | *J. Am. Chem. Soc.* 2012, 134, 5832−5835

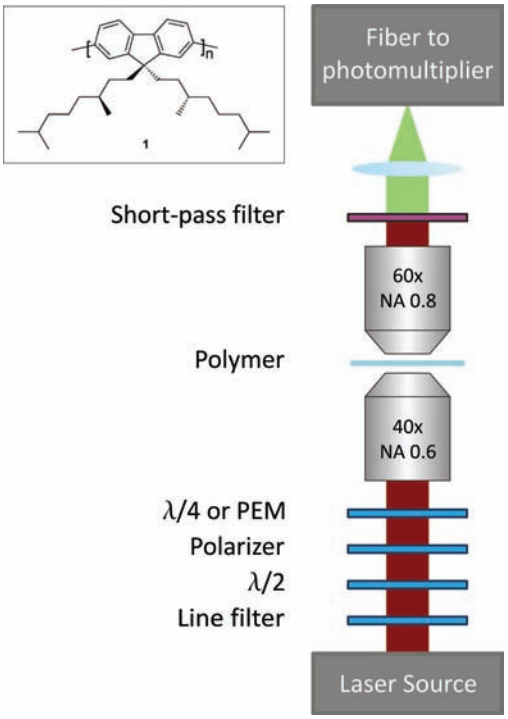

Figure 1. Schematic of the experimental setup (PEM = photoelastic modulator; the line filter is a band-pass filter with a center wavelength at 830 nm for fiber autofluorescence rejection). Inset: Natta projection of polymer **1**.

continuously with annealing time and temperature, eventually leading to the left-handed arrangement extending over the whole film.[8,17,20,21]

2. EXPERIMENTAL DETAILS

To probe the spatial distribution of the CD in such samples, we implemented two different imaging modes, namely, a static mode and a dynamic mode. In the static imaging mode, a quarter-wave ($\lambda/4$) plate is used to excite the sample sequentially with LCP and RCP light. A photomultiplier in counting mode is used as a detector, and two subsequent images for the two circularly polarized states of light are recorded sequentially. Alternatively, in dynamic mode, a photoelastic modulator (PEM) modulates the excitation beam between LCP and RCP at a modulation frequency of 50 kHz. TPF is recorded using a photomultiplier in current mode and lock-in signal demodulation.

The experimental setup for the two types of CD−TPF microscopy is presented in Figure 1. The pulsed laser beam (Chameleon, Coherent Inc.; central wavelength, 830 nm; repetition rate, 80 MHz) first passes through an optical fiber acting as the illumination source of the microscope and then is collimated. Next, after spectral filtering of the laser emission from spurious fluorescence, it is circularly polarized with a zeroth-order $\lambda/4$ plate or, alternatively, modulated by the PEM. The beam is then sent to the sample through a strain-free microscope objective (NA = 0.6, 40×). The pulse duration measured by second-order autocorrelation techniques at the sample plane is estimated to be ~400 fs. The radiation collected by a second strain-free objective (NA = 0.8, 60×) is filtered by a short-pass filter (cutoff at 774 nm) to block the excitation wavelength.

Better sensitivity is obtained in the static mode, since single-photon counting is possible. This mode allows a lower excitation intensity to be used, but it is more sensitive to possible long-term drifts in the laser power that could occur during the acquisition of an image as well as to other mechanical or (photo)chemical instabilities of the setup and sample, respectively. Such effects, however, proved to be negligible in our experiments. The dynamic mode, on the other hand, requires the use of a more complex modulation−demodulation scheme but is less affected by mechanical and power drifts and does not require any postprocessing of the acquired images. In the present CD−TPF microscopy experiments, the two methods yielded similar results on the same area of the sample.

The spatial resolution of our setup, according to the optical features in the TPF maps, is well below 500 nm. Notably, because of the second-order nonlinearity of TPF, the lateral resolution is improved by a factor of $\sqrt{2}$ relative to single-photon-based techniques employing the same wavelength. On the other hand, we used a central wavelength that is twice the one needed to obtain single-photon CD maps, rendering the best obtainable resolution a factor of $\sqrt{2}$ worse than in single-photon CD mapping.

We evaluate the dissymmetry factor of the TPF signals, g_{TPF}, which is defined as[22]

$$g_{TPF} = |g|\exp(-i\phi_{TPF}) = \frac{I_{2L} - I_{2R}}{(I_{2L} + I_{2R})/2} \quad (1)$$

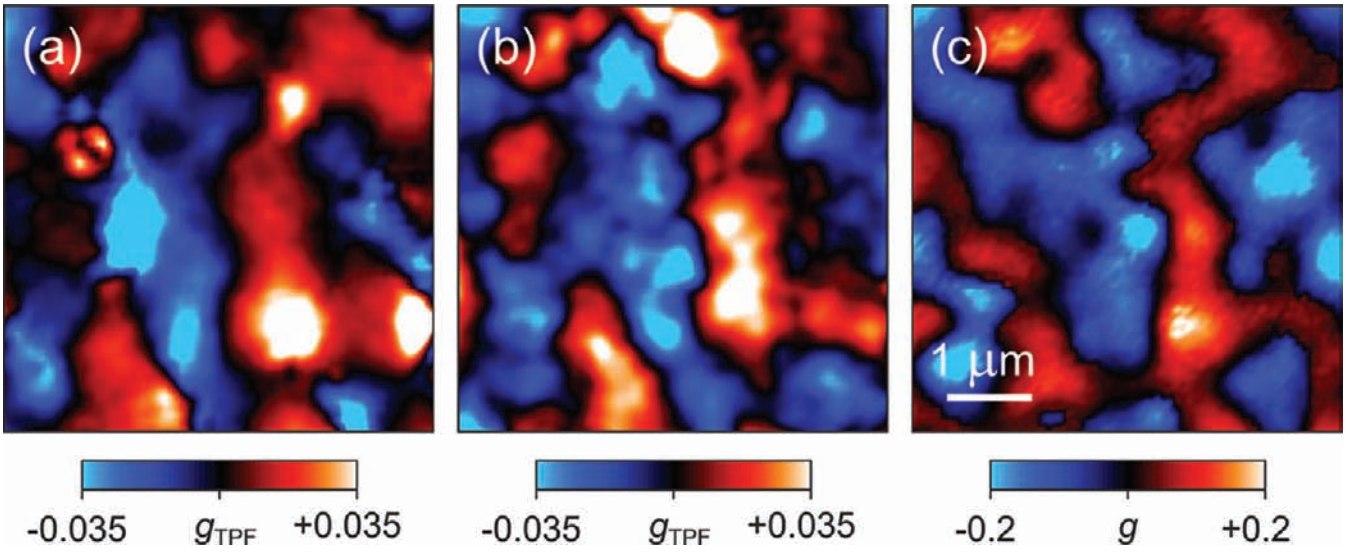

Figure 2. CD in the TPF mapping signal. Shown are maps of (a, b) the dissymmetry factor g_{TPF} for the dichroic TPF signal excited at λ = 830 nm collected in (a) dynamic mode and (b) static mode, and (c) the dissymmetry factor g for the circular dichroic transmission at λ = 405 nm, measured in dynamic mode. Images (a) and (b) have been post-processed using a 2×2 2D Gaussian filter.

dx.doi.org/10.1021/ja209916y | J. Am. Chem. Soc. 2012, 134, 5832−5835

where $I_{2L(R)}$ stands for the TPF intensity excited with LCP (RCP) light. In the dynamic mode, the signal demodulated by the lock-in amplifier is directly proportional to the numerator, while the nondemodulated signal is proportional to the denominator. In the static mode, g_{TPF} is obtained according to eq 1 by dividing the difference between the LC and RC TPF maps by their average. Although similar to the quantity g discussed in ref 10, g_{TPF} addresses the dichroism of a totally different quantity, namely, the excited TPF, rather than the direct transmission, so a direct comparison of these values is not straightforward.

We accurately checked for the presence of possible artifacts deriving from birefringence in the sample or in the optics.[22] Birefringence can in fact produce a spurious dichroism signal in both the dynamic and static modes when the detection path is not sufficiently insensitive to the polarization state of the collected light. We thoroughly evaluated the residual anisotropy of the optics and the detector and were able to conclude that artifacts associated with birefringence amount to variations of g_{TPF} smaller than ±0.003.

3. RESULTS AND DISCUSSION

2D maps of g_{TPF} obtained using both the dynamic and static modes are presented in Figure 2 together with a map of the transmission CD dissymmetry factor g associated with the CD measured for the transmission of light (wavelength, 405 nm; obtained in the dynamic mode).[10] All of the maps were collected in the same region of the sample. As can be inferred from the maps, g_{TPF} displays spatial variations, with $|g_{TPF}|$ ranging between 0 and 0.07, which is more than 1 order of magnitude larger than the detection limit imposed by the remaining anisotropy of the present setup. This result highlights the sensitivity of our apparatus for quantitative evaluation of small chiroptical effects. A contrast in the sign of g_{TPF} for neighboring areas, represented by the blue and red zones in Figure 2, is clearly visible. The capability of CD−TPF microscopy to distinguish between the two different structural chiral configurations underlines its considerable potential for use in various situations where a multiphoton microscopy method provides favorable imaging properties.

Despite the rather low TPF signal, there is a very good agreement between the maps obtained with the two different methods (dynamic and static), as is immediately apparent from a comparison of panels (a) and (b) of Figure 2. The map of transmission CD dissymmetry factor g is presented in Figure 2c. Although $|g|$ is ∼1 order of magnitude larger that $|g_{TPF}|$, the spatial variations of g and g_{TPF} are highly correlated in the three maps in Figure 2, showing dichroic domains[10] with the same sign of their chiroptical response in both the transmission and TPF signals. Such a correlation is not obvious a priori, as g and g_{TPF} describe very different phenomena and might be differently affected by spatial variations of the density and thickness of the polymer film. For instance, g_{TPF} suffers from self-absorption of the fluorescence light by the sample, while g might be influenced by variations of the thickness and possible overlap of domains within the thickness of the film.

Our setup can be readily adapted to measure the linear dichroism (LD) of the sample. This is done by demodulating the measured signal at the second harmonic of the PEM frequency in dynamic mode or by substituting the $\lambda/4$ plate with a $\lambda/2$ plate and collecting successive images with crossed linear light polarizations in the static mode. Figure 3 compares the CD and LD maps obtained by measuring the TPF signal excited at 830 nm. The linear dissymmetry factor lg_{TPF} is defined as the difference of the TPF signals obtained for the two crossed linear polarizations divided by their average.

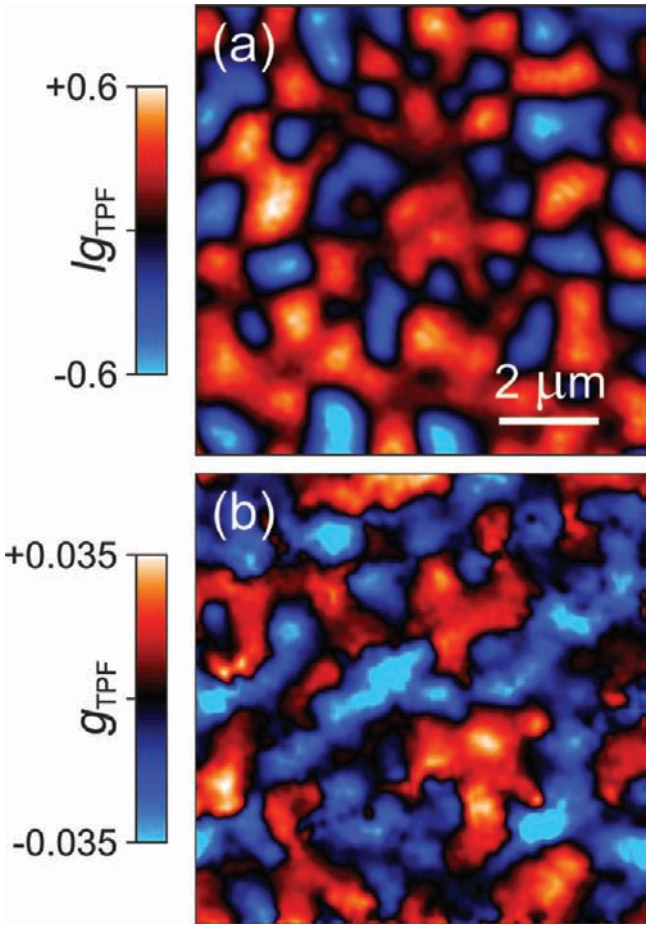

Figure 3. Spatial distributions of (a) the linear dissymmetry ratio lg_{TPF} and (b) the circular dissymmetry ratio g_{TPF} for TPF excited at 830 nm. The two maps were collected at the same sample position.

Notably, the LD exhibited by the sample is much higher than the CD, and the lateral variations of the linear and circular dissymmetry factors are uncorrelated. This observation demonstrates the effectiveness of our apparatus in disentangling linear and circular optical effects, which might exhibit some crosstalk in a less isotropic setup.

We can also exploit a further operation mode available with our setup, consisting of the possibility of acquiring TPF spectra at a fixed sample position using an imaging spectrometer with a back-illuminated CCD. We employed this method to acquire the spectral dependence of the TPF dissymmetry factor for different light polarization states (not shown), which was found to be constant within experimental uncertainties in the 470−750 nm wavelength range. This means that there is basically no difference in the fluorescence spectra once these have been normalized to the absorbed power, the latter being proportional to the fluorescence spectrum integrated over the entire spectral range. Therefore, the dichroic signal seems to be due only to strongly polarization-dependent two-photon absorption, thus justifying the strong correlation that exists between the dissymmetry maps obtained by measuring the transmission at 405 nm and the TPF excited at 830 nm (see Figure 2) with circularly polarized light.

4. CONCLUSION

We have demonstrated the feasibility and versatility of circular dichroism two-photon fluorescence (CD−TPF) microscopy.

dx.doi.org/10.1021/ja209916y | J. Am. Chem. Soc. 2012, 134, 5832−5835

Films of π-conjugated polyfluorene **1** display a sizable dissymmetry factor of the two-photon-excited fluorescence CD. It has been shown that the cholesteric arrangement of this chiral polyfluorene influences the absorption even in the case of a two-photon process, which results in a clearly detectable dichroic signature over the entire film. Using a confocal optical microscope, we were able to detect the 2D spatial distribution of the two-photon CD, visualizing domains with different helical structures.

In perspective, this technique can also be employed to obtain 3D information (e.g., Z-scan or CD−TPF tomography) even without a second pinhole.

AUTHOR INFORMATION

Corresponding Author

marco.finazzi@fisi.polimi.it

Present Addresses

[⊥]Institute for Molecules and Materials, Radboud University, Heyendaalseweg 135, 6525 AJ Nijmegen, The Netherlands.

[#]Institute of Applied Physics, Johannes Kepler University, Altenberger Straße 69, A-4040 Linz, Austria.

Author Contributions

[‖]These authors contributed equally.

Notes

The authors declare no competing financial interest.

ACKNOWLEDGMENTS

Luca Frezza and Stefano Perissinotto are warmly acknowledged for their help in casting the film samples. Financial support by Fondazione Cariplo through the PONDER Project (2009-2726), by MIUR through the PRIN Project (2008J858Y7), and by the European Union (EU) Nano Sci-European Research Associates (ERA) FENOMENA Project is gratefully acknowledged.

REFERENCES

(1) Power, E. A. *J. Chem. Phys.* **1975**, *63*, 1348−1350.

(2) Tinoco, I. Jr. *J. Chem. Phys.* **1975**, *62*, 1006−1009.

(3) Toro, C.; De Boni, L.; Lin, N.; Santoro, F.; Rizzo, A.; Hernandez, F. E. *Chem.—Eur. J.* **2010**, *16*, 3504−3509.

(4) Turner, D. H.; Tinoco, I. Jr.; Maestre, M. *J. Am. Chem. Soc.* **1974**, *96*, 4340−4342.

(5) Tanaka, K.; Pescitelli, G.; Nakanishi, K.; Berova, N. *Monatsh. Chem.* **2005**, *136*, 367−395.

(6) Hernández, F. E.; Rizzo, A. *Molecules* **2011**, *16*, 3315−3337.

(7) Markowicz, P. P.; Samoc, M.; Cerne, J.; Prasad, P. N.; Pucci, A.; Ruggeri, G. *Opt. Express* **2004**, *12*, 5209−5214.

(8) De Boni, L.; Toro, C.; Hernández, F. E. *Opt. Lett.* **2008**, *33*, 2958−2960.

(9) Savoini, M.; Biagioni, P.; Lakhwani, G.; Meskers, S. C. J.; Duò, L.; Finazzi, M. *Opt. Lett.* **2009**, *34*, 3571−3573.

(10) Savoini, M.; Biagioni, P.; Meskers, S. C. J.; Duò, L.; Hecht, B.; Finazzi, M. *J. Phys. Chem. Lett.* **2011**, *2*, 1359−1362.

(11) Denk, W.; Strickler, J. H.; Webb, W. W. *Science* **1990**, *6*, 73−76.

(12) Jeong, B.; Lee, B.; Jang, M. S.; Nam, H.; Yoon, S. J.; Wang, T.; Doh, J.; Yang, B.-G.; Jang, M. H.; Kim, K. H. *Opt. Express* **2011**, *19*, 13089−13096.

(13) Biagioni, P.; Celebrano, M.; Savoini, M.; Grancini, G.; Brida, D.; Mátéfi-Tempfli, S.; Mátéfi-Tempfli, M.; Duò, L.; Hecht, B.; Cerullo, G.; Finazzi, M. *Phys. Rev. B* **2009**, No. 045411.

(14) Oda, M.; Nothofer, H.-G.; Lieser, G.; Scherf, U.; Meskers, S. C. J.; Neher, D. *Adv. Mater.* **2000**, *12*, 362−365.

(15) Craig, M. R.; Jonkheijm, P.; Meskers, S. C. J.; Schenning, A. P. H. J.; Meijer, E. W. *Adv. Mater.* **2003**, *15*, 1435−1438.

(16) Yan, J.-C.; Cheng, X.; Zhou, Q.-L.; Pei, J. *Macromolecules* **2007**, *40*, 832−839.

(17) Tsiminis, G.; Ruseckas, A.; Samuel, I. D. W.; Turnbull, G. A. *Appl. Phys. Lett.* **2009**, *94*, No. 253304.

(18) Biagioni, P.; Celebrano, M.; Zavelani-Rossi, M.; Polli, D.; Labardi, M.; Lanzani, G.; Cerullo, G.; Finazzi, M.; Duò, L. *Appl. Phys. Lett.* **2007**, *91*, No. 191118.

(19) Lakhwani, G.; Gielen, J.; Kemerink, M.; Christianen, P. C. M.; Janssen, R. A. J.; Meskers, S. C. J. *J. Phys. Chem. B* **2009**, *113*, 14047−14051.

(20) Geng, Y. H.; Trajkovska, A.; Katsis, D.; Ou, J. J.; Culligan, S. W.; Chen, S. H. *J. Am. Chem. Soc.* **2002**, *124*, 8337−8347.

(21) Geng, Y. H.; Trajkovska, A.; Culligan, S. W.; Ou, J. J.; Chen, H. M. P.; Katsis, D.; Chen, S. H. *J. Am. Chem. Soc.* **2003**, *125*, 14032−14038.

(22) Tang, Y.; Cook, T. A.; Cohen, A. E. *J. Phys. Chem. A* **2009**, *113*, 6213−6216.